A General Purpose Thermal Model

Barry Rubin,* SPE, Computer Modelling Group
W. Lloyd Buchanan, SPE, Computer Modelling Group

Abstract

This paper describes a fully implicit four-phase (oil, water, gas, solid fuel) numerical reservoir model for simulating hot water injection, steam injection, dry combustion, and wet combustion in one, two, or three dimensions and in either a Cartesian, radial, or curvilinear geometry. The simulator rigorously models fluid flow, heat transfer (convective and conductive), heat loss to formation, fluid vaporization/condensation, and chemical reactions. Any number of oil or gas phase components may be specified, along with any number of solid phase components (fuel and catalysts).

The simulator employs either D4 Gaussian elimination or powerful incomplete factorization methods to solve the often poorly conditioned matrix problems. An implicit well model is coupled to the simulator, where reservoir unknowns and well block pressures are primary variables.

This paper includes (1) comparisons of the numerical model's results with previously reported laboratory physical models' results for steam and combustion and (2) analytical solutions to a hot waterflood problem. In addition, an actual field-scale history match is presented for a single-well steam stimulation problem.

Introduction

Recent papers by Crookston *et al.*,[1] Youngren,[2] Rubin and Vinsome,[3] and Coats[4] have outlined the current trend in thermal process simulation. The trend has been the development of more implicit, more comprehensive finite-difference simulators.

Youngren[2] describes a model based on a highly implicit steam model. The components representing air and combustion gases are treated explicitly. Burning reactions are handled not through rates but through the assumption of 100% oxygen utilization at the combustion front. Crookston *et al.*[1] describe a linearized implicit combustion model that can describe the reaction of a predetermined set of gases and oils. Both of these models are multidimensional and do not handle wellbore-reservoir coupling fully implicitly. Rubin and Vinsome[3] describe a fully implicit one-dimensional (1D) combustion tube simulator. Coats[4] describes a fully implicit four-phase multicomponent multidimensional combustion simulator. This model is general in nature except for the wellbore-reservoir coupling.

This work describes a general, fully implicit, four-phase, multicomponent, multidimensional steam and combustion simulator that includes a fully implicit well model and a suite of powerful iterative techniques that can be used for the solution of large-scale thermal problems.

*Now with BP Resources Canada Ltd.

The following sections of this paper describe the model's fluid and and energy flow equations, property package, powerful iterative techniques capable of reliable use with steam and combustion problems, fully implicit well model, and equation substitution formulation. Further, a section considering the applications of the model is presented.

Mathematical Model

The simulator ISCOM rigorously models fluid flow, vaporization/condensation phenomena, and heat transfer and is efficient enough to allow the simulation of realistically large reservoir problems. The formulation allows for any number of chemical components and reactions. The components can exist in any of four phases: oil, water, gas, or solid. A reaction also can occur in any of the above phases. Furthermore, water and any of the oil components can vaporize.

The simulator development is based on the following assumptions.

1. The model can operate in one, two, or three dimensions (1D, 2D, or 3D) with variable grid spacing.
2. Cartesian, radial, non-Cartesian (variable-thickness grids), and specific curvilinear grids corresponding to the commonly used well patterns can be used.
3. The number of components existing in each phase is variable, and the components can be distributed among four phases.
4. The number and type of chemical reactions can be varied.
5. Each layer, well, or block in the reservoir can exhibit different properties (e.g., viscosities, relative permeabilities, and compressibilities) at different times.
6. Wells can operate under specified fluid rates or flowing pressures and are subject to a hierarchy of user-specified constraints.
7. The simulator must be reasonably efficient to handle field-scale simulation economically, without sacrificing accuracy.

Grid Generation. The model defines a block-centered grid system in 1-, 2-, or 3D, normally based on Cartesian *xyz* coordinates. Radial geometries are accommodated by internal modification of the gridblock volumes and interblock transmissibilities. For rectangular grids with variable thickness layers, the interblock transmissibilities and gravity head terms are derived from gridblock dimensions and depth from reference.

Curvilinear grids are generated by the method of conformal transformation, which yields analytical formulae for potential and stream functions. Two simple patterns are considered: one-eighth of a five-spot and one-eighth of a nine-spot. The method involves finding a complex

function representative of the pattern and setting the potential function equal to the real part and the stream function equal to the imaginary part. Any number of grid points can be used, since the grid is generated automatically. Results of comparisons with five-point and nine-point Cartesian operators indicate that, for the above geometries, grid orientation is eliminated. Further, by using curvilinear grids, far fewer grid points are required to achieve a desired accuracy.

The set of simulator equations is composed of material balance equations for each component, an energy balance equation, equilibrium equations, algebraic constraint equations, and well flow equations.

Material Balance Equations. For water,

$$\Delta T_w^{N+1}(\Delta p_o^{N+1}-\Delta p_{cwo}^{N+1}-g_w^{N+1}\Delta z)$$

$$+\Delta y_m^{N+1}T_g^{N+1}(\Delta p_o^{N+1}+\Delta p_{cgo}^{N+1}-g_g^{N+1}\Delta z)$$

$$+\rho_w^{N+1}q_w^{N+1}+\rho_g^{N+1}y_m^{N+1}q_g^{N+1}+r_m^{N+1}$$

$$=\frac{V_B}{\Delta t}\delta(\phi_F\rho_w S_w+\phi_F y_m\rho_g S_g);\quad m=1. \quad \ldots\ldots\ldots (1)$$

For $n_{cc}-1$ volatile oil components,

$$\Delta x_m^{N+1}T_o^{N+1}(\Delta p_o^{N+1}-g_o^{N+1}\Delta z)$$

$$+\Delta y_m^{N+1}T_g^{N+1}(\Delta p_o^{N+1}+\Delta p_{cgo}^{N+1}-g_g^{N+1}\Delta z)$$

$$+\rho_o^{N+1}x_m^{N+1}q_o^{N+1}+\rho_g^{N+1}y_m^{N+1}q_g^{N+1}+r_m^{N+1}$$

$$=\frac{V_B}{\Delta t}\delta(\phi_F x_m\rho_o S_o+\phi_F y_m\rho_g S_g);\ m=2\ldots n_{cc}.$$

$$\ldots\ldots\ldots\ldots\ldots\ldots\ldots\ldots (2)$$

For n_{cnc} noncondensible gas components,

$$\Delta y_m{}^{N+1}T_g^{N+1}(\Delta p_o^{N+1}+\Delta p_{cgo}^{N+1}-g_g^{N+1}\Delta z)$$

$$+\rho_g^{N+1}y_m^{N+1}q_g^{N+1}+r_m^{N+1}=\frac{V_B}{\Delta t}\delta(\phi_F y_m\rho_g S_g);$$

$$m=n_{cc}+1\ldots n_{cc}+n_{cnc}. \quad \ldots\ldots\ldots\ldots\ldots (3)$$

For n_{cs} solid-phase components,

$$r_m^{N+1}=\frac{V_B}{\Delta t}\delta(\phi_v C_{cm});$$

$$m=n_{cc}+n_{cnc}+1\ldots n_{cc}+n_{cnc}+n_{cs}. \quad \ldots\ldots\ldots (4)$$

Energy Balance Equation. The energy balance equation is

$$\Delta H_w^{N+1}T_w^{N+1}(\Delta p_o^{N+1}-\Delta p_{cwo}^{N+1}-g_w^{N+1}\Delta z)$$

$$+\Delta H_o^{N+1}T_o^{N+1}(\Delta p_o^{N+1}-g_o^{N+1}\Delta z)$$

$$+\Delta H_g^{N+1}T_g^{N+1}(\Delta p_o^{N+1}+\Delta p_{cgo}^{N+1}-g_g^{N+1}\Delta z)$$

$$+\Delta Q_{TC}^{N+1}\Delta T^{N+1}+H_{rxn}^{N+1}+H_{\text{LOSS}}^{N+1}$$

$$+\rho_w^{N+1}H_w^{N+1}q_w^{N+1}+\rho_o^{N+1}H_o^{N+1}q_o^{N+1}$$

$$+\rho_g^{N+1}H_g^{N+1}q_g^{N+1}=\frac{V_B}{\Delta t}\delta[\phi_F\rho_w S_w U_w$$

$$+\phi_F\rho_o S_o U_o+\phi_F\rho_g S_g U_g+(1-\phi_v)\rho_r U_r+\phi_v\rho_c U_c].$$

$$\ldots\ldots\ldots\ldots\ldots\ldots\ldots\ldots (5)$$

Equilibrium Equations. The simulator has oil and hydrocarbon gases, and steam and liquid water in equilibrium. The thermodynamic phase equilibrium conditions are expressed as follows.

For water,

$$y_1^{N+1}=K_1^{N+1}. \quad \ldots\ldots\ldots\ldots\ldots\ldots\ldots (6)$$

For oils,

$$y_m^{N+1}=K_m^{N+1}x_m^{N+1};\ m=2\ldots n_{cc}. \quad \ldots\ldots\ldots\ldots (7)$$

Constraint Equations. The definitions of mole fraction, saturation, and porosity provide the simulator with appropriate constraint equations.

$$\sum_{m=2}^{n_{cc}} x_m^{N+1}=1. \quad \ldots\ldots\ldots\ldots\ldots\ldots\ldots (8)$$

$$\sum_{m=1}^{n_{cc}+n_{cnc}} y_m^{N+1}=1. \quad \ldots\ldots\ldots\ldots\ldots\ldots\ldots (9)$$

$$S_o^{N+1}+S_w^{N+1}+S_g^{N+1}=1. \quad \ldots\ldots\ldots\ldots\ldots\ldots (10)$$

$$\phi_F^{N+1}=$$

$$\phi_v^{N+1}\left[1-\left(\frac{\sum_{m=n_{cc}+n_{cnc}+1}^{n_{cc}+n_{cnc}+n_{cs}} C_{cm}^{N+1}}{\rho_c^{N+1}}\right)\right].$$

$$\ldots\ldots\ldots\ldots\ldots\ldots\ldots\ldots (11)$$

Well Flow Equations. Well flow equations represent production or injection constraints that are solved for

simultaneously, along with reservoir unknowns in gridblocks containing a section of a well.[5] Because the coupling is fully implicit, and since wellbore-reservoir coupling derivatives are included in the Jacobian matrix, the well and reservoir conditions always satisfy the well flow equations. There is no lagging of rate or pressure level.

There are six well flow equations to represent user-specified conditions and 11 user-specified constraints. The rate of production of phase i from layer j of well k is defined as

$$q_{ijk}=I_{ijk}(p_{wf_k}+h_{jk}-p_{ojk}), \quad \ldots\ldots\ldots\ldots\ldots\ldots (12)$$

where I_{ijk} is the layer productivity or injectivity of phase i in layer j of well k, h_{jk} is the pressure drop from the bottomhole to layer j in well k, p_{wf_k} is the bottomhole flowing pressure (BHFP) of well k, and p_{ojk} is the oil phase pressure in the gridblock containing layer j of well k. Capillary pressure has been neglected.

When rates at stock-tank conditions are required, the molar flow rate of each component is calculated as feed to a flash module. The flash module calculates stock-tank rates and derivatives. Stock-tank-condition phase specifications and derivatives analogous to Eq. 12 are obtained.

In all cases, derivatives of well indices (I) are taken with respect to all reservoir variables. Normally, I_{ijk} is a function of phase or total mobility. The head term is taken to be explicit in time. Although this reduces the implicitness of the well model calculation, we have never encountered difficulty with this assumption.

We can describe the six well flow conditions as variations of Eq. 12.

1. For a *shut-in well,*

$$\sum_j \sum_{i=o,w,g} I_{ijk}^{N+1}(p_{wf_k}^{N+1}+h_{jk}^{N}-p_{ojk}^{N+1})=0. \quad \ldots (13)$$

2. For a *constant-total-volume injection well,*

$$q_{Tk}-\sum_j \sum_{i=o,w,g} I_{ijk}^{N+1}(p_{wf_k}^{N+1}+h_{jk}^{N}-p_{ojk}^{N+1})=0,$$

$$\ldots\ldots\ldots\ldots\ldots\ldots\ldots\ldots (14)$$

where q_{Tk} is the specified total injection rate and I_{ijk} is the injectivity of phase i from layer j of well k.

3. For a *constant-pressure injection or production well,*

$$p_{wfs}-p_{wf_k}^{N+1}=0, \quad \ldots\ldots\ldots\ldots\ldots\ldots (15)$$

where p_{wfs} is the specified value of either injection or production flowing pressure and p_{wf_k} is the actual bottomhole pressure (BHP) of well k.

4. For a *constant-oil-rate production well,*

$$q_{ok}-\sum_j I_{ojk}^{N+1}(p_{wf_k}^{N+1}+h_{jk}^{N}-p_{ojk}^{N+1})=0, \quad \ldots\ldots (16)$$

where q_{ok} is the total flow of oil from well k.

5. For a *constant-gas-rate production well,*

$$q_{gk}-\sum_j I_{gjk}^{N+1}(p_{wf_k}^{N+1}+h_{jk}^{N}-p_{ojk}^{N+1})=0. \quad \ldots\ldots (17)$$

6. For a *constant-liquid-rate production well,*

$$q_{Lk}-\sum_j (I_{wjk}^{N+1}+I_{ojk}^{N+1})(p_{wf_k}^{N+1}+h_{jk}^{N}-p_{ojk}^{N+1})=0,$$

$$\ldots\ldots\ldots\ldots\ldots\ldots\ldots\ldots (18)$$

where q_{Lk} is the specified liquid production rate for well k.

As a control feature, the well equations described above can be replaced by constraint equations. The appropriate replacement occurs when any one of a chosen list of constraints is violated. The constraints can be applied in a user-specified priority if multiple constraint violations occur. Two examples of the constraints are the *maximum water/oil ratio,* given by

$$\sum_j [I_{wjk}^{N+1}-(F_{wo_k})I_{ojk}^{N+1}](p_{wf_k}^{N+1}+h_{jk}^{N}-p_{ojk}^{N+1})=0,$$

$$\ldots\ldots\ldots\ldots\ldots\ldots\ldots\ldots (19)$$

and the *maximum water rate,* given by

$$\sum_j I_{wjk}^{N+1}(p_{wf_k}^{N+1}+h_{jk}^{N}-p_{ojk}^{N+1})-F_{w_k}=0. \quad \ldots\ldots (20)$$

The constraints presently accommodated are (1) maximum water/oil ratio, (2) maximum gas/oil ratio, (3) maximum water/gas ratio, (4) maximum gas rate, (5) maximum water rate, (6) maximum BHP, (7) minimum BHP, (8) minimum oil rate, (9) minimum gas rate, (10) maximum oxygen concentration, and (11) maximum wellbore temperature.

Normally, Constraints 1, 2, 3, 10, and 11 cannot be applied once they are violated; instead, they are used to signal that the well be shut in or that the run be terminated. The other constraints can be used as well-operating conditions, as well as shut-in or termination criteria.

Eqs. 1 through 18 represent a set of coupled partial difference and algebraic equations that relate p_o, S_w, S_o, T, x_m where $m=2\ldots n_{cc}$, y_m where $m=1\ldots n_{cc}+n_{cnc}$, and C_{cm} where $m=n_{cc}+n_{cnc}+1\ldots n_{cc}+n_{cnc}+n_{ncs}$, for each gridblock, as well as p_{wf_k} where $k=1\ldots n_w$, for each well.

Direct and Iterative Solution Procedures

The above sets of equations are solved in ISCOM by using combinations of direct, sequential, and iterative methods.

1. Gaussian elimination with D4 ordering[6] can be specified for all unknowns.

2. D4 Gaussian elimination can be specified on a subset of unknowns, followed by a sequential or iterative solution of the remaining unknowns.[7]

3. The entire matrix can be solved using iterative procedures.[8]

The development of efficient iterative routines capable of solving the often poorly conditioned system of equations encountered during the simulation of thermal processes is crucial. With three or more unknowns per gridblock, even 3D problems with 1,000 gridblocks cannot be solved efficiently with D4 Gaussian elimination.

It is well known that, for single-phase problems that give rise to symmetric positive definite systems, standard iterative methods, such as line-successive overrelaxation (LSOR), often fail when encountering large permeability contrasts.[9-11] For these problems, incomplete factorization methods are the most efficient.[9,11,12] The incomplete factorization methods also can be used to solve problems where off-diagonal elements are larger than diagonal elements.[13,14] These methods can be generalized for the strongly nonsymmetric block-banded systems arising in thermal simulation and have been proven effective.[7,15] The techniques employed by ISCOM consist of incomplete factorizations accelerated by Orthomin.[7,8]

Several options are incorporated into the solution package. It is possible to vary the degree of factorization, that is, the number of extra bands that are positioned to contain nonzero elements resulting from elimination. Further, it is possible to reorder the matrix before performing the factorization. One particularly successful ordering is D4. With a matrix reordered by using D4, it is possible to iterate only on the D4-reduced system. It is important to note that with these methods the work per block step increases very slowly with increasing problem size. Appendix A illustrates the power of these methods. A Jacobian from an $11\times11\times8$ 3D steam problem (three equations per gridblock) was run on the CRAY 1 computer. Appendix A shows the performance of the iterative options. Run times of the iterative routines and D4 Gaussian elimination are presented, with and without vectorization.

Well Model Solution

As previously mentioned, the reservoir conservation equations and well flow equations are solved together fully implicitly. The Jacobian resulting from this coupled system can be partitioned into the form shown in Eq. 21.

$$\begin{pmatrix} J_{11} & J_{12} \\ J_{21} & J_{22} \end{pmatrix} \begin{pmatrix} \delta X_1 \\ \delta X_2 \end{pmatrix} = - \begin{pmatrix} b_1 \\ b_2 \end{pmatrix}, \quad \ldots\ldots\ldots\ldots\ldots\ldots (21)$$

where

δX_1 = change in reservoir unknowns,
δX_2 = change in bottomhole pressures,
b_1 = conservation equation residual, and
b_2 = wellflow equation residual.

Here J_{11} is the standard matrix of fluid and energy conservation derivatives taken with respect to reservoir variables (block pressure, temperature, saturations, and mole fractions); J_{12} represents the derivatives of the mass or energy sink or source terms taken with respect to BHP's; J_{21} contains the derivatives of well flow equations with respect to reservoir variables; and J_{22} contains the derivatives of well flow equations with respect to BHP's.

J_{12} and J_{21} implicitly couple the reservoir unknowns to the wellbore unknowns (BHP). The entire partitioned matrix system is solved simultaneously to satisfy both reservoir conservation equations and wellbore constraints. Appendix B describes the solution of the partitioned matrix in more detail.

Unknown and Equation Alignment

In this section, the conversion of the multicomponent four-phase problem into a minimum set of equations and unknowns is discussed.

The coke concentration, C_c, is used instead of the solid-phase saturation to obtain the coke (or solid phase component) in place. Coke concentration relates the void porosity, ϕ_v, to the fluid porosity, ϕ_F, thus accounting for the volume of the solid phase.

In general, a volume, V, of a reservoir will contain a volume of water, V_w; oil, V_o; gas, V_g; solid phase, V_c; and rock, V_r, so that

$$V=V_w+V_o+V_g+V_c+V_r. \quad \ldots\ldots\ldots\ldots\ldots (22)$$

We can define a fluid volume, V_F, so that

$$V_F=V_w+V_o+V_g=V_v-V_c, \quad \ldots\ldots\ldots\ldots\ldots (23)$$

where $V_v=V-V_r$ is void volume and fluid porosity

$$\phi_F=\left(\frac{V_F}{V}\right)=\left(\frac{V_v}{V}\right)\cdot\left(\frac{V_v-V_c}{V_v}\right)=\phi_v\left(1-\frac{V_c}{V_v}\right), \quad \ldots\ldots\ldots\ldots\ldots\ldots\ldots (24)$$

where ϕ_v is the void porosity V_v/V.

V_c/V_v is the fraction of the void volume occupied by coke and is equal to C_c/ρ_c, so that

$$\phi_F=\phi_v(1-C_c/\rho_c). \quad \ldots\ldots\ldots\ldots\ldots\ldots (25)$$

Therefore, $V_j=S_j\phi_F V$, $j=o,w,g$, and

$$V_c=\frac{C_c}{\rho_c}\phi_v V. \quad \ldots\ldots\ldots\ldots\ldots\ldots (26)$$

It is crucial to align each unknown with a material balance, energy balance, or constraint, in which the derivative of the unknown is prominent in the equation's diagonal. This reduces the need for pivoting and can allow for faster convergence of nonlinear problems.

The distribution of each component among the four phases is presented in Fig. 1. The variables for the system shown in Fig. 1 are solved using the following mass/energy balances and constraints.

Case A: With Noncondensible Gas. Pressure is aligned with the total noncondensible gas conservation equation. Water saturation is aligned with the water conservation equation. Oil saturation is aligned with the sum of oil conservation equations. Temperature is aligned with the energy conservation equation. The $n_{cc}-2$ oil-phase mole fractions are solved for by using the corresponding $n_{cc}-2$ oil component conservation equations. The

Component		Phase			
Number	Name	Water	Oil	Gas	Solid
1	Water	1		y_1	
2 • • • n_{cc}	Oil_1 $Oil_{n_{cc}-1}$		x_2 • • • $x_{n_{cc}}$	y_2 • • • $y_{n_{cc}}$	
$n_{cc}+1$ • • • $n_{cc}+n_{cnc}$	Gas_1 $Gas_{n_{cnc}}$			y_{ncc+1} • • • $y_{n_{cc}+n_{cnc}}$	
$n_{cc}+n_{cnc}+1$ • • • $n_{cc}+n_{cnc}+n_{cs}$	$Solid_1$ $Solid_{n_{cs}}$				c_{c1} • • • $c_{cn_{cs}}$

Fig. 1—Distribution of components in the four phases.

$(n_{cc}-1)$th oil mole fraction is obtained by difference (Eq. 8). The $n_{cnc}-1$ noncondensible gas mole fractions are solved by using the corresponding $n_{cnc}-1$ gas conservation equations. The n_{cnc}th gas mole fraction is obtained by difference (Eq. 9). The n_{cs} solid phase concentrations are solved for by using n_{cs} solid-phase conservation equations.

Case B: Without Noncondensible Gas. When $n_{cnc}=0$, the pressure is aligned with the water conservation equation when a gas phase is not present. When a gas phase is present, pressure is aligned with the constraint

$$\sum_{m=1}^{n_{cc}} y_m = 1. \quad \ldots\ldots\ldots\ldots\ldots\ldots\ldots\ldots (27)$$

The water saturation is solved using the saturation constraint

$$S_o + S_w = 1 \quad \ldots\ldots\ldots\ldots\ldots\ldots\ldots\ldots (28)$$

when a gas phase is not present, and with the water conservation equation when a gas phase is present. The remaining unknowns, $n_{cc}-1$ oil molar fractions, oil saturation, temperature, and n_{cs} solid-phase concentrations, are solved for as in Case A.

Constraints that are violated during an iteration, that is,

$$\sum_{m=1}^{n_{cc}} y_m < 1 \text{ or } S_o + S_w > 1, \quad \ldots\ldots\ldots\ldots\ldots (29)$$

are replaced by the appropriate constraint equation on the next iteration. Since the constraints involve variables within one gridblock (no interblock coupling), the Jacobian matrix is modified to eliminate the constraint.

Timestep Selection

The simulator contains an error-controlling timestep selector. A full description of the algorithm and its properties is given in Ref. 16. Two estimations are made of the current time rate of change of the primary reservoir variables. The first is given by the backwards time difference formula[17]

$$(D_a - \Delta t D_f)\left(\frac{\mathrm{d}}{\mathrm{d}t}X\right) = F. \quad \ldots\ldots\ldots\ldots\ldots\ldots\ldots\ldots (30)$$

The second is a calculation based on the current flow rates into each block:

$$D_a\left(\frac{\mathrm{d}}{\mathrm{d}t}X\right) = F. \quad \ldots\ldots\ldots\ldots\ldots\ldots\ldots\ldots (31)$$

The difference between these two rates for any reservoir variable estimates the current reservoir nonlinearity. Lindberg's work[18] describes how to translate this estimate into an appropriate timestep size. The first calculation is not costly if matrix factorizations are saved, and the second only involves inverting the block diagonal matrix D_a. The method also can be used to predict the proper timestep size after a well is shut in or put on line.

The algorithm produces estimates of truncation errors (i.e., errors in pressure, saturations, and temperature) that correlate well with the user input value of tolerable error. As well as increasing accuracy, the use of the optimal timestep sequence generally reduces running time on most problems by approximately 20%, and on some specific test problems by as much as 70%.

Property Package

The ISCOM fluid and reservoir property package is being updated continually to provide the most realistic physical properties available. However, many property calculations are similar to previously published packages[1,4]; hence, only more novel applications of recent methods or correlations are described. In particular, the unique approach of Carlson[19] for evaluating nonwetting phase hysteresis and the calculation of temperature-dependent relative permeabilities and capillary pressures are discussed. The reaction model also is described briefly.

Relative Permeability and Capillary Pressure. The simulator accepts oil/water and liquid/gas relative permeability and capillary pressure tables corresponding to reference temperature T_1 and normalizes the saturation entries.

$$S_{wD}=\frac{S_w-S_{wc}}{1-S_{orw}-S_{wc}} \quad \ldots\ldots\ldots\ldots\ldots\ldots\ldots\ldots (32)$$

and

$$S_{LD}=\frac{1-S_g-S_{wc}-S_{org}}{1-S_{gc}-S_{wc}-S_{org}}. \quad \ldots\ldots\ldots\ldots\ldots\ldots (33)$$

Temperatures T_1 and T_2 (the second corresponding to a high steam or combustion temperature) are entered along with values for S_{wc}, S_{orw}, S_{gc}, and S_{org} at the two temperatures. When Eqs. 32 and 33 are used to calculate S_{wD} and S_{LD} from S_w and S_g, to perform a table search, the critical saturations are assumed to vary linearly with temperature between T_1 and T_2; they are not allowed outside the range defined by the input values. In this way, S_{wD} and S_{LD} are temperature dependent.

Also, the relative permeability table values can be scaled up or down with temperature. The endpoint values of the k_{row}, k_{rog}, k_{rw}, and k_{rg} curves are entered for temperatures T_1 and T_2. The relative permeability obtained from table search then is scaled for temperature T; for example,

$$k_{rw}(T)=k_{rw}(S_{wD})\left[1+\frac{k_{rw}(T_2)-k_{rw}(T_1)}{T_2-T_1}(T-T_1)\right].$$

Below T_1 and above T_2 no further correction is applied. Either the first or second model of Stone can be used to obtain k_{ro} from k_{row} and k_{rog}.

These normalized saturations can be applied to the calculation of capillary pressure, as well. The capillary pressure, permeability, and surface tension are related by the Leverett J-function:

$$\sqrt{\frac{p_{cop}k}{\sigma_{op}\phi}}=J(S_p),\ p=w,g. \quad \ldots\ldots\ldots\ldots\ldots (34)$$

If we assume the J-function is equivalent to our normalized saturations, the water and gas capillary pressures are calculated from

$$\sqrt{\frac{p_{cow}k}{\sigma_{ow}\phi}}=S_{wD} \quad \ldots\ldots\ldots\ldots\ldots\ldots\ldots (35)$$

and

$$\sqrt{\frac{p_{cog}k}{\sigma_{og}\phi}}=S_{LD}. \quad \ldots\ldots\ldots\ldots\ldots\ldots\ldots (36)$$

The surface tensions are allowed to change linearly with temperature between two input values $\sigma_{op}(T_1)$ and $\sigma_{op}(T_2)$:

$$\sigma_{op}(T)=\sigma_{op}(T_1)+\left[\frac{\sigma_{op}(T_2)-\sigma_{op}(T_1)}{T_2-T_1}\right](T-T_1),$$

$$p=w,g. \quad \ldots\ldots\ldots\ldots\ldots\ldots\ldots (37)$$

Relative Permeability Hysteresis. The hysteresis option available for the nonwetting phase in either the oil/water or the oil(liquid)/gas two-phase system is Carlson's[19] development of Land's[20] method and is applied to the normalized system.

Land's law, which is empirically based, states that S_{nwi} and S_{nwr} are related by the following.

$$\frac{1}{S_{nwr}}-\frac{1}{S_{nwi}}=C_{rf}, \quad \ldots\ldots\ldots\ldots\ldots\ldots (38)$$

where

S_{nwi} = saturation of nonwetting phase when switching from drainage to imbibition or imbibition to drainage,

S_{nwr} = saturation of nonwetting phase at which the imbibition branch attains $k_{rnw}=0$, and

C_{rf} = rock fluid property constant.

We have generalized this relation to include interior points as well as the endpoints of the imbibition branch:

$$\frac{1}{S_{nwr}-S_{nw}+k_{rnwd}^{-1}(k_{rnw})}-\frac{1}{k_{rnwd}^{-1}(k_{rnw})}=C_{rf}, \quad (39)$$

where the drainage data are represented as $k_{rnw}=k_{rnwd}(S_w)$ and the inverse function $k_{rnwd}^{-1}(k_{rnw})$ implies the saturation S_{nw}. Carlson's extension of Land's law allows the calculation of C_{rf} from drainage data and two or more points on a common imbibition curve.

Once C_{rf} is known, Carlson's formulation allows the computation of the imbibition branch relative permeability of the nonwetting phase given the values of the current nonwetting phase saturation S_{nw} and the current imbibition branch as designated by S_{nwi}.

ISCOM can be used to calculate the value of C_{rf} from drainage and imbibition data or can accept a user input value. Details of the calculation of C_{rf} are given in Carlson.[19]

Reaction Model. Each reaction between the $n_{cc}+n_{cnc}+n_{cs}$ components, a_i, is represented by

$$\sum_i \lambda_{ki}a_i=\sum_i \lambda_{ki}^{*}a_i;\ k=1\ldots n_r. \quad \ldots\ldots\ldots\ldots (40)$$

TABLE 1—DATA FOR LAUWERIER HOT FLUID PROBLEM

Reservoir length, m	10
Grid type	1D, linear
Number of gridblocks	20
Cross-sectional area, m^2	1
Water saturation	1
Initial temperature, °C	5
Water viscosity, mPa·s	1
Water *K*-value	0
Water molecular weight, g/gmol	1
Water mole density, gmol/m^3	1
Water molar heat capacity, J/gmol·K	1
Rock volumetric heat capacity, J/m^3·K	1
Rock and water thermal conductivity, J/m·d·K	0
Overburden volumetric heat capacity, J/m^3·K	1
Overburden thermal conductivity, J/m·d·K	1
Injection data	
Fluid	water
Rate, m^3/d	1
Temperature, °C	6
Quality	0
Relative permeability data	$k_{rw}=S_w$

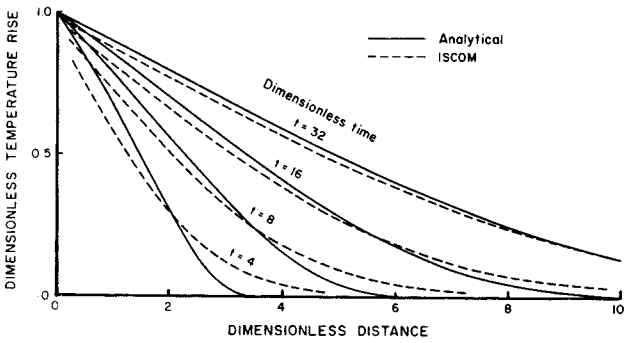

Fig. 2—Dimensionless temperature profiles for the Lauwerier hot fluid problem.

If a component reacts in several phases, a reaction must be specified for each phase in which the reaction occurs. The rate of reaction, R_k, is expressed as

$$R_k=A_k(e^{-E_{ak}/RT})\pi(F_{\rho jm})^{e_m}, \quad \ldots\ldots\ldots\ldots\ldots (41)$$

where the index m encompasses all reacting components with nonzero stoichiometric coefficients on the left side of Eq. 40. The density factors, $F_{\rho jm}$, are

$$F_{\rho jm}=\phi_F\rho_j x_{jm}S_j, \quad \ldots\ldots\ldots\ldots\ldots\ldots\ldots (42)$$

where $j=w,o,g$ for water, oil, and gas phases, x_{jm} is the mole fraction of component m in phase j, and S is saturation. The one exception is the oxygen component, which may be expressed as

$$F_{\rho jm}=p_{O_2}, \quad \ldots\ldots\ldots\ldots\ldots\ldots\ldots\ldots (43)$$

the partial pressure of oxygen, if desired. For the coke phase, $F_{\rho cm}$ is equal to $\phi_v C_{cm}$.

Applications

Lauwerier Hot Fluid Problem. Lauwerier[21] obtained an analytical solution to a 1D hot fluid injection problem

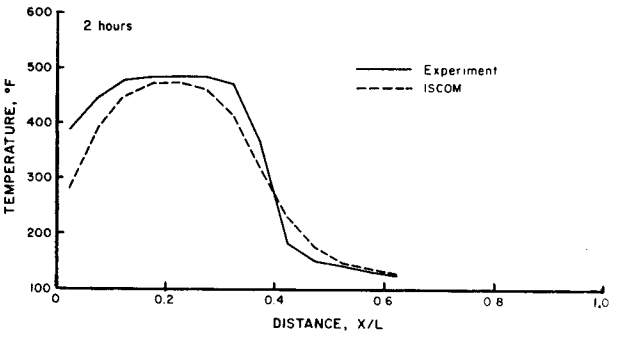

Fig. 3—Combustion tube temperature profiles at 2 hours.

in which most of the injected heat is lost to the surrounding rock. This is essentially what happens when a hot fluid (steam or water) invades a narrow channel, such as a fracture or a high-permeability stratum. Lauwerier showed that the solution to the problem depends on four dimensionless groups. These are t_D, dimensionless time; L_{D2}, dimensionless distance along the channel; L_{D1}, dimensionless distance perpendicular to the channel; and γ, the ratio of volumetric specific heat of the channel to that of the overburden.

The same dimensionless problem was solved using ISCOM with data given in Table 1. The ratio γ is assumed to be 1. The porosity and permeability values used are immaterial to the dimensionless problem. The heat loss calculation of Vinsome and Westerveld[22] was used.

The temperature profiles obtained by ISCOM are compared with the analytical solutions at four dimensionless times in Fig. 2. The discrepancy between the analytical and the numerical curves results from the simulator's single-point upstream weighting of the convection term, which tends to reduce the temperature gradient. This amount of dispersion is normal for this gridblock size. By integrating the heat loss rate over the reservoir length, the rate of heat loss for the entire reservoir is obtained. Even at early times there is significant cancellation of the error introduced by numerical dispersion. This means that the total reservoir heat loss rate and, therefore, the total cumulative heat lost to the overburden given by the simulator are quite reliable despite the effect that numerical dispersion has on the temperature profiles.

Combustion Tube Example: Smith and Perkins. This example illustrates how the thermal model solves a typical combustion tube experimental problem. The test is that of Smith and Perkins[23] and is a wet forward combustion of 0.845-g/cm^3 [36°API] oil in a vertical tube. The data set reported by Coats[4] was used directly (Tables 2 through 4); no changes were made to the data to obtain a better match with the experimental results. Twenty gridblocks were used to describe the tube.

The temperature profiles obtained are compared with the experimental profiles at 2 and 6 hours, in Figs. 3 and 4. The numerical model has correctly predicted the position of the combustion front and the temperature level behind it. The high temperatures at the trailing edge of the experimental profile, however, are not obtained. This probably is caused by heat convecting back up the trailing edge, as reported in Smith and Perkins.[23]

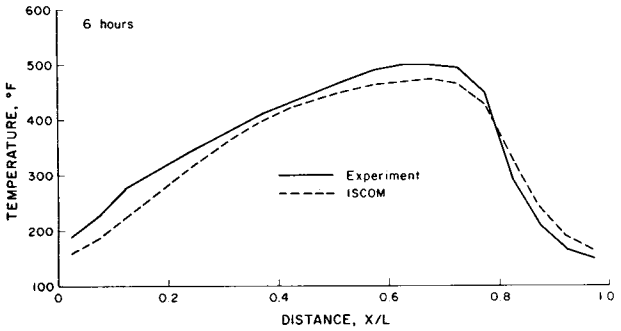

Fig. 4—Combustion tube temperature profiles at 6 hours.

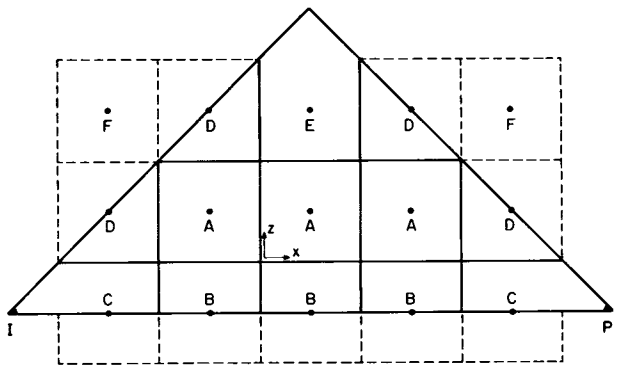

Fig. 5—5×3 grid used to represent the triangular geometry.

The decreased slope of the numerical temperature gradient at the combustion front is caused by numerical dispersion. This amount of dispersion is normal for single-point upstream mobility and enthalpy weighting of flow terms, for this grid size.

Dead Oil Steam Injection Example. The laboratory 3D dead oil steam injection experiment reported by Coats *et al.*[24] was simulated using the multiblock well model coupled to the simulator. The reservoir consists of a box 0.305 m [12 in.] square and 0.163 m [6.4 in.] high with injection and production perforated tubing at opposite corners. Owing to symmetry, only half of this volume is simulated. The resulting triangular prism is represented by a 5×3×4 vertical cross section grid. The 5×3 grid used for the triangular geometry in the horizontal *x-z* plane is shown in Fig. 5. The dotted lines represent the block dimensions entered so that the grid nodes (block centers) fall as shown. The gridblock volumes and areas are modified to obtain the block boundaries denoted by the solid lines. The vertical *y*-direction is described by four equal-thickness layers. There is overburden and underburden packed next to the model, but no material adjacent to the sides, to approximate a repeated pattern. The reservoir and fluid properties are given in Tables 5 through 8. The fluids considered are water and a heavy, nonvolatile oil. For water, internal vapor pressure and steam tables are used.

Fig. 6 shows equal-temperature contours in the plane lying between the two wells, at 10, 30, and 70 minutes. An adequate match between the numerical and experimental temperature contours is obtained. Again, numerical dispersion tends to reduce the temperature gradient, causing the 300°F [149°C] contour to be retarded. The grid shown in Fig. 5 is particularly useful here because a plane of nodes lies on the plane of interest.

TABLE 2—DATA FOR COMBUSTION TUBE PROBLEM

Combustion Tube Description	
Tube length, m	1.753
Tube orientation	vertical
Cross-sectional area, m^2	0.007748
Porosity	0.25
Permeability, m^2	6.91×10^{-13}
Rock heat capacity, J/m^3-K (Temperature in K)	$1.607 \times 10^6 - 2257T$
Rock thermal conductivity, J/m-d-K	4.49×10^5
Initial Conditions	
Pressure, kPa	5620
Temperature, K	
Top 20% of tube	533
Bottom 80% of tube	322
Water, oil, gas saturation	0.3, 0.4, 0.3
Oil phase composition (by moles)	
Heavy oil	0.0840
Medium oil	0.2063
Light oil	0.7097
Gas phase composition (by moles)	
Inert gas	0.71
Oxygen	0.29
Relative Permeability and Capillary Pressure	
Critical water saturation	0.25
Residual oil saturation in water/oil system	0.25
Residual oil saturation in liquid/gas system	0.09
Critical Gas Saturation	0
Capillary pressure	0

$S_{ew} = (S_w - 0.25)/(1 - 0.25 - 0.25)$
$S_{eg} = (S_g - 0.0)/(1 - 0.25 - 0.09 - 0.0)$
$k_{rw} = 0.5\ (S_{ew})^2$
$k_{row} = 1.0\ (1 - S_{ew})^2$
$k_{rog} = 1.0\ (1 - S_{eg})^2$
$k_{rg} = 1.0\ (S_{eg})^2$

Reactions*,**

Heavy oil (HO) burning:
$HO + 45.17\ O_2 \rightarrow 29.71\ H_2O + 37.46\ CO_x + 1.89 \times 10^7$ J/gmol HO
Rate, gmol HO reacted/d/m^3:
$3.08 \times 10^5 \exp(-E_a/RT)(\phi \rho_o S_o x_2)^2 (p_g y_6)$
Medium oil (MO) burning:
$MO + 25.08\ O_2 \rightarrow 16.5\ H_2O + 20.8\ CO_x + 1.05 \times 10^7$ J/gmol MO
Rate, gmol MO reacted/d/m^3:
$2.55 \times 10^4 \exp(-E_a/RT)(\phi \rho_o S_o x_3)^2 (p_g y_6)$
Light oil (LO) burning:
$LO + 11.66\ O_2 \rightarrow 7.67\ H_2O + 9.67\ CO_x + 4.89 \times 10^6$ J/gmol LO
Rate, gmol LO reacted/d/m^3:
$3.65 \times 10^4 \exp(-E_a/RT)(\phi \rho_o S_o x_4)^2 (p_g y_6)$

Injection and Production Scheme

Injection (top of tube)
1. From beginning to end of run, inject 3.060 m^3/d air (standard conditions).
2. Beginning at 0.02 days, inject 0.00883 m^3/d water along with the air.

Production (bottom of tube)
Constant pressure production at 5620 kPa from open end.

* R = Gas constant.
T = Temperature (K).
E_a = Activation energy (76 200 J/gmol).
**Mole fraction subscripts refer to component numbers in Table 3.

TABLE 3—COMPONENT PROPERTIES

	Symbol	Molecular Weight	Critical Pressure (kPa)	Critical Temperature (K)	Vapor Heat Capacity (J/gmol·K)	Vapor Viscosity (kPa·d)
1. Water	H_2O	18	22106	647.4	default	$1.295\times10^{-16}T^{1.075}$
2. Heavy oil	HO	508.9	349.6	887.8	1278	—
3. Medium oil	MO	282.6	1117	767.2	709.9	9.259×10^{-13}
4. Light oil	LO	131.4	2321	562.8	330	3.472×10^{-13}
5. Inert gas	CO_x	32	5171	194.4	30.28	$3.719\times10^{-15}T^{0.702}$
6. Oxygen	O_2	32	5033	154.4	32.15	$3.883\times10^{-15}T^{0.721}$

TABLE 4—COMPONENT LIQUID PROPERTIES

	Standard Density (kg/m^3)	Mole Density ($gmol/m^3$)	Compressibility (1/kPa)	Thermal Expansion (1/K)	Vaporization Enthalpy (J/gmol)	Viscosity (kPa·d)	Equilibrium *K*-Value
Water	1000	55 500	1.45×10^{-6}	9.0×10^{-4}	default	default	default
Heavy oil	979.5	1925	1.45×10^{-6}	6.84×10^{-4}	0	$1.157\times10^{-13}e^{2727/T}$	0
Medium oil	906.6	3208	1.45×10^{-6}	6.84×10^{-4}	0	$3.208\times10^{-13}e^{1868/T}$	$(2.144\times10^{7}/p)\cdot e^{-7567/T}$
Light oil	719.2	5474	1.45×10^{-6}	6.84×10^{-4}	0	$4.144\times10^{-13}e^{1186/T}$	$(5.287\times10^{6}/p)\cdot e^{-4628/T}$

TABLE 5—DATA FOR STEAM PROBLEM

Description of Physical Model	
Model dimensions, m	$0.305\times0.305\times0.163$
Grid used	$5\times4\times3$ vertical cross section
Porosity	0.3063
Permeability, m^2	2.122×10^{-10}
Rock heat capacity, $J/m^3\cdot K$	2.59×10^{6}
Rock thermal conductivity, $J/m\cdot d\cdot K$	1.50×10^{5}
Overburden heat capacity, $J/m^3\cdot K$	2.68×10^{6}
Overburden thermal conductivity, $J/m\cdot d\cdot K$	1.05×10^{6}
Rock compressibility, 1/kPa	4.4×10^{-7}
Rock thermal expansion, 1/K	0
Initial Conditions	
Pressure, kPa	482.6
Temperature, K	297.0
Water, oil, gas saturation	0.179, 0.821, 0.0
Reference pressure, kPa	482.6
Reference temperature, K	297.0
Injection and Production	
Injection	
$0.053\ m^3/d$ cold water equivalent of 468.5 K, 69.7%-quality steam is injected into the bottom two layers by means of a constant-rate multiblock injection well.	
Production	
Production is from the entire thickness by means of a four-layer constant-pressure multiblock production well with BHP (bottom layer) of 482.6 kPa. The well consists of a perforated tube, 0.0016 m in radius.	

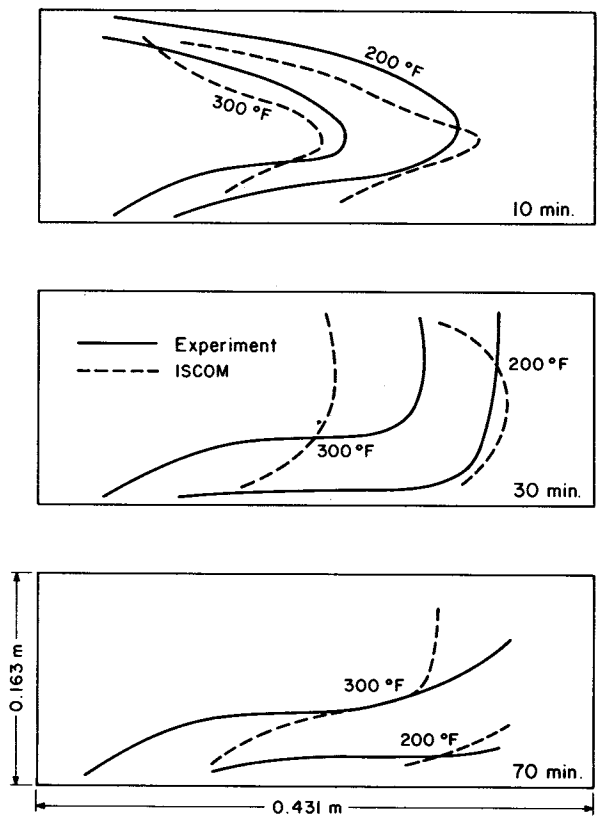

Fig. 6—Temperature contours in plane between wells.

Field-Scale Example: Cyclic Steam Injection. One typical application of a thermal reservoir simulator is to predict the performance of a cyclic steam injection project. Matching the water and oil production for one isolated cycle may be possible by manipulating a few key parameters. However, much less success has been obtained in matching many cycles in different wells using a single recovery model with consistent parameter values. Geshelin and Grabowski[25] incorporated a fracture model in a modified version of ISCOM but could not match a first-year history with a reasonable number of trials.

Ito[26] has had more success using a sand deformation model. A modified version of ISCOM was used to test this concept, and one example of a successful match of several consecutive cycles is shown here. The heavy oil reservoir (1 to 4 Pa·s [1,000 to 4,000 cp]) is less than 10 m [33 ft] thick and is worked only a few months each year; two of these production periods are examined here. The reservoir was represented by a 15×9 areal grid, and three wells were incorporated into the grid.

A good history match was obtained for all three wells for four production periods. Figs. 7 and 8 are the pro-

TABLE 6—COMPONENT PROPERTIES

	Molecular Weight	Stock Tank Density (kg/m^3)	Liquid Mole Density ($gmol/m^3$)	Liquid Compressibility (1/kPa)	Liquid Thermal Expansion (1/K)	Liquid Heat Capacity (J/gmol·K)	Vapor Viscosity (kPa·d)
Water	18	1000	55 500	4.5×10^{-7}	8.8×10^{-4}	default	$2.72\times10^{-16}T^{1.075}$
Heavy oil	500	963	1925	7.3×10^{-7}	7.2×10^{-4}	1047	—

TABLE 7—RELATIVE PERMEABILITIES AND CAPILLARY PRESSURES*

S_w	k_{rw}	k_{row}	S_L	k_{rg}	k_{rog}
0.130	0.0000	1.0000	0.200	0.1700	0.0000
0.191	0.0051	0.9990	0.395	0.1120	0.0294
0.250	0.0102	0.7690	0.433	0.1022	0.0461
0.294	0.0168	0.7241	0.515	0.0855	0.0883
0.357	0.0275	0.6206	0.569	0.0761	0.1172
0.414	0.0424	0.5040	0.614	0.0654	0.1433
0.490	0.0665	0.3714	0.663	0.0500	0.1764
0.577	0.0970	0.3029	0.719	0.0372	0.2170
0.630	0.1148	0.1555	0.750	0.0285	0.2255
0.673	0.1259	0.0956	0.805	0.0195	0.2919
0.719	0.1381	0.0576	0.850	0.0121	0.3373
0.789	0.1636	0.0000	0.899	0.0026	0.5169
1.000	1.0000	0.0000	1.000	0.0000	1.0000

*$p_{cow} = 0$
$p_{cog} = 0.8618 - 0.8618(S_L)$

TABLE 8—LIQUID VISCOSITIES

Temperature (K)	Water Viscosity (10^{-11} kPa-d)	Oil Viscosity (10^{-11} kPa-d)
297.0	1.079	6690.0
310.9	0.7928	1597.0
338.7	0.4977	216.4
366.5	0.3565	54.40
394.3	0.2662	20.14
422.0	0.2106	9.84
449.8	0.1850	6.02
533.2	0.1406	2.89

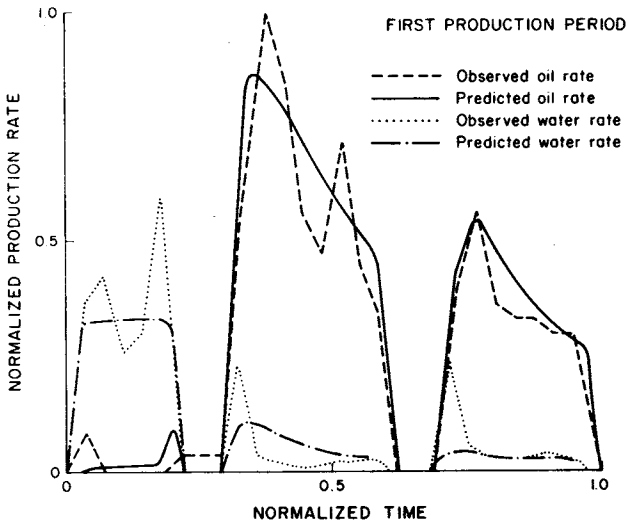

Fig. 7—Steam stimulation history match: first production period.

duction histories of one well for the first and third periods. The horizontal axis is time normalized by the length of the production period, and the vertical axis is production rate normalized by the maximum observed oil rate for the period.

Computing Times. The computing time for the Lauwerier problem is trivially small and so is not reported. Further, the computing time for the cyclic steam injection problem is not available. The statistics for the Smith and Perkins combustion tube problem and dead oil steam injection problem are presented below.

	Grid	Timesteps	Running Time (Honeywell DPS8) (CPU minutes)
Combustion tube	20×1×1	44	5.68
Dead oil steam	5×3×4	67	17.0

Summary

The general purpose thermal model described here extends the wellbore-reservoir coupling normally found in reservoir simulators. Well flow equations, governing injection and production, and reservoir flow equations are solved simultaneously. The simulator makes use of powerful incomplete factorization iterative methods to allow the practical solution of large problems. The model is general in nature and can solve the dead oil problem, as well as the compositional thermal problem. The model operates in three dimensions and in various coordinate systems (i.e., Cartesian, radial, and curvilinear). The results of four simulations are presented. In all cases, simulator and experimental/field results compared well.

Nomenclature

A_k = pre-exponential reaction constant
b_1 = right-side vector
C_{cm} = concentration of component m in coke (solid phase) $gmol/m^3$ [lbm mol/cu ft]
C_{rf} = rock fluid property constant for hysteresis model, dimensionless
d/dt = time derivative
D_a = Jacobian of accumulation terms
D_f = Jacobian of flow terms
E_a = activation energy, J/gmol [Btu/lbm mol]
F = matrix of flow terms
F_w = maximum water rate factor, m^3/d [cu ft/D]

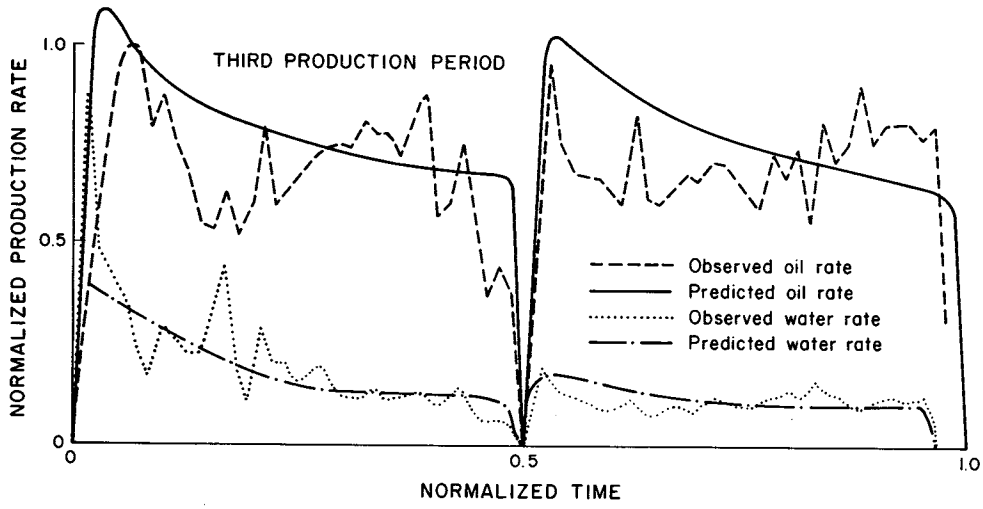

Fig. 8—Steam stimulation history match: third production period.

F_{wo} = water/oil ratio, dimensionless
$F_{\rho jm}$ = density factor of component m in phase j, gmol/m^3 [lbm mol/cu ft]
g_j = pressure gradient resulting from gravity in phase j, kPa/m [psi/ft]
h_{jk} = head of layer j in well k, kPa [psi]
H_j = enthalpy of phase j, J/gmol [Btu/lbm mol]
H_{LOSS} = heat loss to adjacent formation, J/d [Btu/D]
H_{rxn} = enthalpy added by reactions, J/d [Btu/D]
I_{ijk} = well index of phase i, layer j, well k, m^3/kPa·d [cu ft/psi-D]
J = Jacobian matrix
$J(s)$ = Leverett J-function, dimensionless
k = absolute permeability, md
k_{rj} = relative permeability of phase j, dimensionless
K_m = K-value of component m $(=y_m/x_m)$, dimensionless
L_{D1} = dimensionless length
L_{D2} = dimensionless length
n_{cc} = number of condensible components
n_{cnc} = number of noncondensible components
n_{cs} = number of solid-phase components
n_r = total number of reactions
n_w = total number of wells
p_{coj} = capillary pressure of phase j, $j=w,g$, kPa [psi]
p_j = pressure of phase j, kPa [psi]
p_{O_2} = oxygen partial pressure, kPa [psi]
p_{wf} = bottomhole flowing pressure of well, kPa [psi]
p_{wfs} = p_{wf} specified by user, kPa [psi]
q_{ijk} = volumetric flow rate of phase i, from layer j, of well k, m^3/d [cu ft/D]
q_j = volumetric flow rate of phase j, m^3/d [cu ft/D]
Q_{TC} = flow of energy resulting from thermal conductivity, J/d [Btu/D]
r_m = rate of appearance of component m resulting from all reactions, gmol/d [lbm mol/D]
R_k = rate of reaction k, gmol/m^3·d [lbm mol/cu ft-D]
S_{gc} = critical gas saturation
S_j = saturation of phase j
S_{jD} = normalized saturations
S_{org} = residual oil saturation in the oil/gas system
S_{orw} = residual oil saturation in the oil/water system
S_{wc} = critical water saturation
t = time, days
t_D = dimensionless time
T = temperature, K [°F]
T_j = transmissibility of phase j, m^3/kPa·d [cu ft/psi-D]
U_j = internal energy of phase j, J/gmol [Btu/lbm mol]
V = volume, m^3 [cu ft]
x = oil-phase mole fraction
X,Y = vectors of unknowns
y = gas-phase mole fraction
z = depth from reference, m [ft]
Δ,δ = finite-difference operators
δX = change in vector of unknowns (X)
γ = ratio of heat capacities, dimensionless
λ = stoichiometric coefficient of reactant, dimensionless
λ^* = stoichiometric coefficient of product, dimensionless
π = product operator
ρ_j = mole density of phase j, gmol/m^3 [lbm mol/cu ft]
σ_{oj} = surface tension between oil and phase j, $j=w,g$, N/m^2 [lbf/sq ft]
ϕ = porosity

Subscripts

B = gridblock
c = coke, solid phase
d = drainage
F = fluid
g = gas
L = liquid
m = component number
nw = nonwetting
o = oil
r = rock, residual
v = void
w = water

Superscript

N = timestep number

Acknowledgments

This research is supported by the members of the Computer Modelling Group. We thank A. Au, A. Behie, P. Forsyth, P. Sammon, and G.G. Ford for their helpful comments on this work. We also thank Gulf Canada Resources for permitting us to present the results of their history match simulations.

References

1. Crookston, R.B. *et al.*: "A Numerical Simulation Model for Thermal Recovery Processes," *Soc. Pet. Eng. J.* (Feb. 1979) 37-58.
2. Youngren, G.K.: "Development and Application of an In-Situ Combustion Reservoir Simulator," *Soc. Pet. Eng. J.* (Feb. 1980) 39-51.
3. Rubin, B. and Vinsome, P.K.W.: "The Simulation of the In Situ Combustion Process in One Dimension Using a Highly Implicit Finite-Difference Scheme," *J. Cdn. Pet. Tech.* (Oct./Dec. 1980) 68-76.
4. Coats, K.H.: "In-Situ Combustion Model," *Soc. Pet. Eng. J.* (Dec. 1980) 533-54.
5. Trimble, R.H. and McDonald, A.E.: "A Strongly Coupled, Fully Implicit, Three-Dimensional, Three-Phase Well Coning Model," *Soc. Pet. Eng. J.* (Aug. 1981) 454-58.
6. Price, H.S. and Coats, K.: "Direct Methods in Reservoir Simulation," *Soc. Pet. Eng. J.* (June 1974) 295-308; *Trans.*, AIME, **257**.
7. Behie, A. and Vinsome, P.K.W.: "Block Iterative Methods for Fully Implicit Reservoir Simulation," paper SPE 9303 presented at the 1980 SPE Annual Technical Conference and Exhibition, Dallas, Sept. 21-24.
8. Behie, A. and Forsyth, P.A.: "Incomplete Factorization Methods for Fully Implicit Simulation of Enhanced Oil Recovery," *J. Scientific and Statistical Computing* (Sept. 1984) 343-561.
9. Kershaw, D.S.: "The Incomplete Cholesky Conjugate Gradient Method for the Iterative Solution of Systems of Linear-Equations," *J. Computational Physics* (1978) **26**, 43-65.
10. Stone, H.L.: "Iterative Solution of Implicit Approximations of Multi-Dimensional Partial Differential Equations," *SIAM J. Numerical Analysis* (1968) **5**, 530-58.
11. Watts, J.W.: "A Conjugate Gradient-Truncated Direct Method for the Solution of the Reservoir Simulation Pressure Equation," *Soc. Pet. Eng. J.* (June 1981) 345-53.
12. Meijerink, J.A. and van der Vorst, H.A.: "An Iterative Solution Method for Linear Systems in Which the Coefficient Matrix Is a Symmetric M-Matrix," *Mathematics of Computation* (1977) **31**, 148-62.
13. Behie, G.A. and Forsyth, P.A.: "Comparison of Fast Iterative Methods for Symmetric Systems," *IMA J. Numerical Analysis* (1983) **3**, 41-63.
14. Elman, H.C.: "Preconditioned Conjugate-Gradient Methods for Non-Symmetric Systems of Linear Equations," *Advances in Computer Methods for Partial Differential Equations—IV*, R. Vitchnevetsky and R.F. Stepleman (eds.), IMACS, Rutgers U., New Brunswick, NJ (1981) 409-17.
15. Tan, T.B.S. and Letkeman, J.P.: "Application of D4 Ordering and Minimization in an Effective Partial Matrix Inverse Iterative Method," paper SPE 10493 presented at the 1982 SPE Symposium on Reservoir Simulation, New Orleans, Jan. 31-Feb. 3.
16. Sammon, P.H. and Rubin, B.: "Practical Control of Timestep Selection in Thermal Simulation," paper SPE 12268 presented at the 1983 SPE Symposium on Reservoir Simulation, San Francisco, Nov. 15-18.
17. Mehra, R.K., Hadjitofi, M., and Donnelly, J.K.: "An Automatic Timestep Selector for Reservoir Models," paper SPE 10496 presented at the 1982 SPE Symposium on Reservoir Simulation, New Orleans, Jan. 31-Feb. 3.
18. Lindberg, B.: "Characterization of Optimal Step-Size Sequences for Methods for Stiff Differential Equations," *SIAM J. Numerical Analysis* (1977) **14**, 859-87.
19. Carlson, F.M.: "Simulation of Relative Permeability Hysteresis to the Nonwetting Phase," paper SPE 10157 presented at the 1981 SPE Annual Technical Conference and Exhibition, San Antonio, Oct. 5-7.
20. Land, C.S.: "Calculation of Imbibition Relative Permeability for Two- and Three-Phase Flow from Rock Properties," *Soc. Pet. Eng. J.* (June 1968), 149-56; *Trans.*, AIME, **243**.
21. Lauwerier, H.A.: "The Transport of Heat in an Oil Layer Caused by the Injection of Hot Fluids," *Appl. Sci. Res.*, Martinus Nijhoff, Publisher, The Hague (1955) **5**, Sec. A, No. 2-3, 145-50.
22. Vinsome, P.K.W. and Westerveld, J.: "A Simple Method for Predicting Cap and Base Rock Heat Losses in Thermal Reservoir Simulators," *J. Cdn. Pet. Tech.* (July/Sept. 1980) 87-90.
23. Smith, F.W. and Perkins, T.K.: "Experimental and Numerical Simulation Studies of the Wet Combustion Recovery Process," *J. Cdn. Pet. Tech.* (July/Sept. 1973) 44-54.
24. Coats, K.H. *et al.*: "Three-Dimensional Simulation of Steamflooding," *Soc. Pet. Eng. J.* (Dec. 1974) 573-92; *Trans.*, AIME, **257**.
25. Geshelin, B.M. and Grabowski, J.W.: "Source Distributed Fracture Model for the Numerical Modelling of Oil Sands Steam Simulation," paper SPE 10508 presented at the 1982 SPE Symposium on Reservoir Simulation, New Orleans, Jan. 31-Feb. 3.
26. Ito, Y.: "The Introduction of the Microchannelling Phenomenon to Cyclic Steam Stimulation and Its Application to the Numerical Simulator (Sand Deformation Concept)," *Soc. Pet. Eng. J.* (Aug. 1984) 417-30.
27. George, A.: "On Block Elimination for Sparse Linear Systems," *SIAM J. Numerical Analysis* (1974) **11**, 585-603.

APPENDIX A

Iterative Routine Performance on CRAY 1 Computer

The problem studied is a 3D steam problem with $11 \times 11 \times 8$ gridblocks and three equations per block; total unknowns involved are 2,904.

This example was run using (1) D4 Gaussian elimination, (2) naturally ordered second-degree incomplete factorization,[8] and (3) D4 ordered first-degree incomplete factorization. The iterative cases were run twice, once with combinative preconditioning[7] and once without. All

TABLE A-1—3D STEAM PROBLEM

Solution Method	No Compiler Vectorization (Cray CPU seconds)	Compiler Vectorization (Cray CPU seconds)
Natural second degree	9.18	5.11
D4 first degree	4.12	2.11
Natural second degree and combinative	3.07	1.76
D4 first degree and combinative	3.05	1.41
D4 Gaussian elimination	24.5	5.1

cases were completed and run once in unvectorized mode and once in vectorized mode. The results are listed in Table A-1. See Behie and Forsyth[8] for complete details of the problem. Clearly, the results show that Gaussian elimination vectorizes most efficiently. However, large savings in run time still can be achieved by using incomplete factorizations with combinative preconditioning.

APPENDIX B

Solution of the Partitioned Jacobian Matrix

The partitioned Jacobian system that is to be solved is

$$\begin{pmatrix} J_{11} & J_{12} \\ J_{21} & J_{22} \end{pmatrix} \begin{pmatrix} X_1 \\ X_2 \end{pmatrix} = \begin{pmatrix} b_1 \\ b_2 \end{pmatrix}, \quad \ldots\ldots\ldots\ldots\ldots\ldots \text{(B-1)}$$

where X_1 represents the reservoir variables and X_2 represents the well variables (BHP's). The system of equations B-1 is factored according to one of the methods presented by George[27]—i.e.,

$$\begin{pmatrix} J_{11} & J_{12} \\ J_{21} & J_{22} \end{pmatrix} = \begin{pmatrix} L_1 U_1 & 0 \\ J_{21} & L_2 \end{pmatrix} \begin{pmatrix} I & V \\ 0 & U_2 \end{pmatrix}, \quad \ldots\ldots\ldots \text{(B-2)}$$

where $J_{11}=L_1U_1$, $V=U_1^{-1}L_1^{-1}J_{12}$, and $L_2U_2=J_{22}-J_{21}V$.

This factorization has the advantage that existing solution routines—i.e., direct elimination or iterative methods[7] for solving the reservoir flow system of equations

$$J_{11}X_1=b_1 \quad \ldots\ldots\ldots\ldots\ldots\ldots\ldots\ldots \text{(B-3)}$$

can be expanded to solve the "bordered" system, Eq. B-1. The only extra storage needed is that for V, L_2, and U_2.

The complete algorithm for solving Eq. B-1 can be written as follows.

1. Factor

$$J_{11}=L_1U_1. \quad \ldots\ldots\ldots\ldots\ldots\ldots\ldots\ldots \text{(B-4)}$$

2. Calculate

$$V=U_1^{-1}L_1^{-1}J_{12}. \quad \ldots\ldots\ldots\ldots\ldots\ldots \text{(B-5)}$$

3. Calculate

$$E=J_{22}-J_{21}V. \quad \ldots\ldots\ldots\ldots\ldots\ldots\ldots \text{(B-6)}$$

4. Factor

$$E=L_2U_2. \quad \ldots\ldots\ldots\ldots\ldots\ldots\ldots\ldots \text{(B-7)}$$

5. Solve

$$L_1U_1Y_1=b_1 \quad \ldots\ldots\ldots\ldots\ldots\ldots\ldots \text{(B-8)}$$

for Y_1.

6. Solve

$$L_2Y_2=b_2J_{21}Y_1 \quad \ldots\ldots\ldots\ldots\ldots\ldots\ldots \text{(B-9)}$$

for Y_2.

7. Solve

$$U_2X_2=Y_2 \quad \ldots\ldots\ldots\ldots\ldots\ldots\ldots\ldots \text{(B-10)}$$

for X_2.

8. Calculate

$$X_1=Y_1-VX_2. \quad \ldots\ldots\ldots\ldots\ldots\ldots\ldots \text{(B-11)}$$

If the solution option chosen is direct elimination, L_1 need not be stored. If the solution option chosen is an iterative method, Steps 5 through 8 are repeated until convergence is achieved.

SI Metric Conversion Factors

Btu	× 1.055 056	E+03	=	J
cp	× 1.0*	E+00	=	mPa·s
cu ft	× 2.831 685	E−02	=	m^3
ft	× 3.048*	E−01	=	m
°F	(°F−32)/1.8		=	°C
°F	(°F+459.67)/1.8		=	K
md	× 9.869 233	E−10	=	m^2
psi	× 6.894 757	E+00	=	kPa

*Conversion factor is exact.

SPEJ

Original manuscript received in the Society of Petroleum Engineers office April 12, 1983. Paper accepted for publication Nov. 14, 1983. Revised manuscript received April 30, 1984. Paper (SPE 11713) first presented at the 1983 SPE California Regional Meeting held in Ventura March 23–25.